Production of negative ions on graphite surface in H2/D2 plasmas: experiments and SRIM calculations

Production of negative ions on graphite surface in H2/D2 plasmas: Experiments and srim calculations

G. Cartry, L. Schiesko, C. Hopf, A. Ahmad, M Carrère et al.

Citation: Phys. Plasmas **19**, 063503 (2012); doi: 10.1063/1.4725188
View online: http://dx.doi.org/10.1063/1.4725188
View Table of Contents: http://pop.aip.org/resource/1/PHPAEN/v19/i6
Published by the American Institute of Physics.

Production of negative ions on graphite surface in H_2/D_2 plasmas: Experiments and SRIM calculations

G. Cartry,[1,a)] L. Schiesko,[2] C. Hopf,[2] A. Ahmad,[1] M Carrère,[1] J. M. Layet,[1] P. Kumar,[3] and R. Engeln[4]

[1]*Aix-Marseille University, CNRS, PIIM, UMR 6633, Centre Scientifique de Saint Jérôme, Case 241, 13397 Marseille Cedex 20, France*
[2]*Max-Planck-Institut für Plasmaphysik, EURATOM Association, Boltzmannstr. 2, 85748 Garching, Germany*
[3]*Inter University Accelerator Centre (IUAC), New Delhi 110067, India*
[4]*Department of Applied Physics, Eindhoven University of Technology, Eindhoven, The Netherlands*

(Received 26 March 2012; accepted 12 April 2012; published online 13 June 2012)

In previous works, surface-produced negative-ion distribution-functions have been measured in H_2 and D_2 plasmas using graphite surfaces (highly oriented pyrolitic graphite). In the present paper, we use the SRIM software to interpret the measured negative-ion distribution-functions. For this purpose, the distribution-functions of backscattered and sputtered atoms arising due to the impact of hydrogen ions on a-CH and a-CD surfaces are calculated. The SRIM calculations confirm the experimental deduction that backscattering and sputtering are the mechanisms of the origin of the creation of negative ions at the surface. It is shown that the SRIM calculations compare well with the experiments regarding the maximum energy of the negative ions and reproduce the experimentally observed isotopic effect. A discrepancy between calculations and measurements is found concerning the yields for backscattering and sputtering. An explanation is proposed based on a study of the emitted-particle angular-distributions as calculated by SRIM. © *2012 American Institute of Physics*. [http://dx.doi.org/10.1063/1.4725188]

I. INTRODUCTION

The ITER project and its successor DEMO (first nuclear-fusion based power plant prototype) aim at demonstrating power production by magnetic confinement nuclear fusion. Plasma start-up and continuous operation in the case of a tokamak reactor require very efficient heating and non-inductive current drive systems. Neutral beam injection (NBI) which uses high power beams of fast neutral atoms of hydrogen isotopes to heat the plasma is a promising candidate. In most existing NBI systems on contemporary fusion experiments, a beam of positive ions is extracted from a conventional ion source, accelerated to energies of the order of 100 keV and neutralized via charge exchange in a background of neutral hydrogen. Due to the much larger physical dimensions, the NBI systems for both ITER and DEMO require neutral beam energies in the 1 to 2 MeV range where the neutralization of positive ions becomes very inefficient and only the negative ions can be neutralized with sufficient yield. Hence the development of high current negative ion sources (50 A D– beam for ITER) is crucial to the development of the ITER and DEMO NBI systems. The high-current-density negative-ion source for ITER (Ref. 1) is currently the subject of intense research ranging from experimental characterization[2] and modeling of the plasma[3–5] to cesium (Cs) management,[6,7] and negative ion extraction.[8–11]

In high density plasma-based negative-ion sources, D^- negative ions originate from the interaction of a low work function metal surface with ions and neutrals[12,13] from the plasma. The low work function of the surface is usually obtained by Cs deposition on the metal and allows for an efficient electron transfer from the metal to the incident particle and increases noticeably the negative-ion surface-production yield. The high-density negative ion source of ITER is planned to operate with Cs. However, despite its efficiency, this technique presents major drawbacks, such as problematic long-term operational stability, Cs pollution of the accelerator stage, and high Cs consumption, that may disqualify its application for DEMO and strongly complicate ion source operation on ITER. Thus, high-intensity Cs-free negative-ion-source development would be highly desirable for next generation neutral beam injectors. Previous works have shown that graphite could be used as a negative-ion enhancer material in H_2 or D_2 plasmas. The present paper deals with negative ion surface production on graphite material (HOPG, highly oriented pyrolitic graphite) in Cs-free plasmas. Other negative-ion production mechanisms, such as volume production (see for instance Refs. 14–16), are not considered in the present article.

Negative ion formation on graphite is also of interest for understanding and describing the physics occurring at the edge of the fusion plasma, in the vicinity of the divertor. Carbon-fiber-composites (CFC) are used in many tokamaks as divertor material. Negative ion production on the carbon tiles has to be considered to correctly account for the heat load received by the divertor.[17–19] Indeed, the mutual neutralization of H^- and H^+ and the subsequent molecular radiation participate in the heat load balance.

There is a quite important literature on negative ion surface-production in well-controlled beam-experiments at grazing incidence (or low incidence angle), for a large

a)Author to whom correspondence should be addressed. Electronic mail: gilles.cartry@univ-amu.fr.

variety of incident energy, various ion type, and a large variety of surfaces, including caesiated (see, for instance, Refs. 20–25 and references therein) and non-caesiated surfaces (see, for instance, Refs. 26–36 and references therein). H– surface-production on HOPG or polycrystalline graphite has for instance been studied in Refs. 37–40. On the contrary, few works deal with negative ion surface-production in cesium-free plasmas.[41–68] Most of them are related to the industrial process of layer deposition by sputtering and concern mainly oxygen negative ions.[44–58] H– surface-production in Cs-free plasmas has been mainly studied in Refs. 59–62 (carbon materials), Ref. 63 (stainless steel), and Refs. 64–68 (barium surfaces).

Our previous works were focused on H- and D- negative ion production on HOPG surfaces in H_2 and D_2 plasmas.[60–63] The positive ions impinging the surface were H_2^+ and H_3^+ (D_2^+ and D_3^+) with energies in the range of 10 to 150 eV. Surface-produced negative-ion energy-distribution functions were recorded, and the surface-production mechanisms were determined. It has been shown that negative ions are formed by two mechanisms (i) backscattering of an incident particle as a negative ion and (ii) sputtering of an adsorbed hydrogen (deuterium) atom as a negative ion. The dependences of the negative ion yield on positive ion energy and ion type have been studied. The aim of the present paper is to acquire a better understanding of the negative ion surface-production mechanisms in a cesium-free plasma. To this aim, we make use of the SRIM software[69] to calculate backscattered and sputtered neutral distribution functions (NDFs) and yields upon positive hydrogen (deuterium) ion bombardment of a-CH (a-CD) layers.

II. EXPERIMENTS

The experimental set-up was previously described.[60,70,71] Briefly, an HOPG surface is centered in the diffusion chamber of a low-pressure helicon plasma reactor. H_2 or D_2 plasmas are generated, either in capacitive or inductive mode, and the sample is negatively biased with respect to plasma potential by a dc power supply. Positive ions from the plasma strike the sample with an energy $E_0 = e(V_p - V_s)$ where Vs and Vp are sample and plasma potential, respectively. Negative ions formed on the HOPG surface under positive ion bombardment are accelerated by the sheath toward the plasma and gain the energy E_0. Under the low-pressure conditions considered here, they cross the plasma without any collision and reach an energy-resolved mass spectrometer (Hiden EQP300) where they are detected. The mass spectrometer measures the total energy of the negative ion, $E_T = E_{ki} - eV_s$, where E_{ki} is the kinetic energy of the negative ion emitted by the surface. In the following, the negative ion distribution functions (IDFs) are represented as a function of the negative ion's kinetic energy inside the plasma, $E_{kp} = E_{ki} + E_0 = E_{ki} + e(V_p - V_s) = E_T + eV_p$. The plasma potential V_p is deduced from the positive ion distribution function measured by the mass spectrometer. For instance, if the plasma potential is V_p and the surface potential is V_s, a negative ion produced at rest on the surface enters the plasma with a kinetic energy equal to $E_0 = e(V_p - V_s)$ and appears at E_0 on the IDF plot. Therefore, the measured IDFs represent the kinetic energy distribution functions of the surface-produced negative ions shifted by E_0. An example of such a distribution function is shown in Figure 1.

It can be observed that most of the negative ions have energy higher than E_0, showing they have been formed on the surface with an initial energy. By studying these negative ion distribution functions, it was possible to determine the mechanisms of the surface-production of negative ions.[59–61]

The first mechanism is the backscattering of a positive ion as a negative ion (see a scheme of this process in Figure 1 of Ref. 61). According to this mechanism, the maximum energy of a negative ion in the plasma is determined by the nature of the positive ion impinging the surface. Indeed, when an H^+ positive ion, i.e., a proton, is backscattered as an H^- negative ion, the maximum energy transferred to the negative ion is equal to the positive ion's initial energy E_0, assuming in a first approximation that no energy is transferred to the surface. Therefore, the maximum energy of the negative ion in the plasma is equal to $E_1 = 2E_0$. In the case of molecular positive-ion bombardment (H_2^+, H_3^+), dissociation takes place before backscattering. The initial positive-ion energy is shared between the fragments and the maximum energy transferred to the negative ion is equal to $E_0/2$ (H_2^+ bombardment) or $E_0/3$ (H_3^+ bombardment). Therefore, the maximum energy of the negative ion in the plasma is $E_2 = 3/2E_0$ (H_2^+ bombardment) and $E_3 = 4/3E_0$ (H_3^+ bombardment). By varying the positive-ion population in the plasma, it was shown that the H^- maximum energy is always in agreement with the backscattering mechanisms: close to E_1 when the H^+ density is non-negligible, close to E_2 when H^+ density is negligible and H_2^+ density non negligible, and close to E_3 when H^+ and H_2^+ densities are negligible. In other words, the negative-ion maximum energy is determined by the lighter non-negligible positive ion. It was demonstrated that the backscattering mechanism explains at least the tail of the negative ion distribution functions. The same mechanism is also involved in D^- surface production but an isotopic effect has been observed,[61] the D^- negative ion maximum energy being always slightly lower than the expected value (E_1, E_2, or E_3). This can qualitatively be

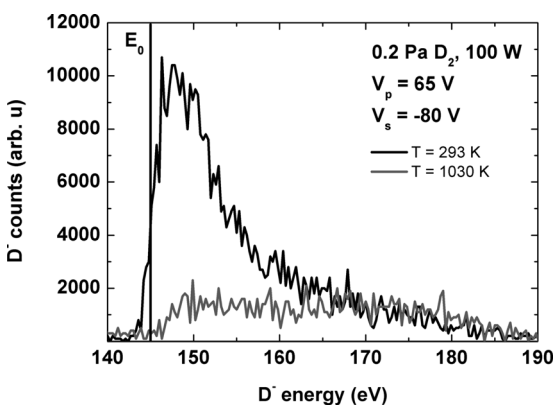

FIG. 1. D^- negative ion distribution function measured at 0.2 Pa in a 100 W D_2 plasma for a sample bias of −80 V, and for two surface temperatures (black: 293 K, grey: 1030 K). The plasma potential is 65 V. $E_0 = e(V_p - V_s)$ is the energy gained in the sheath by the surface-produced negative ions.

explained by invoking the better energy transfer in a binary collision between deuterium and carbon than between hydrogen (H) and carbon. Due to the lower mass difference, deuterium positive ions transfer more energy to the surface and less energy is transferred to the created negative-ion.

The second mechanism is the sputtering of an adsorbed hydrogen atom by an incoming positive ion. It is known that when graphite is heated to high temperature, hydrogen is desorbed. This effect was seen in experiments where the distribution function of surface-produced negative ions was measured while the graphite surface was heated to 1000 K. A strong decrease of the signal (see Figure 1) was observed and it was concluded that at room temperature most of the negative ions are created by sputtering of adsorbed hydrogen atoms since in the absence of adsorbed species (high temperature) the signal is largely reduced. Furthermore, an almost perfect coincidence between IDFs' energetic tails at low and high temperature was observed (see Figure 1). As the energetic tail was previously attributed to negative ions created by the backscattering mechanism, it was deduced that (i) backscattering is the only mechanism producing negative ion at high temperature and (ii) sputtering production dominates over backscattering production at low temperature. Then, it follows that the negative-ion distribution function measured at high temperature represents a backscattered negative-ion distribution function. If it is further assumed that the backscattering mechanism is temperature independent because the high-energy tails at high and low temperature coincide, then subtracting the high-temperature measurements from the low-temperature measurements gives the sputtering negative-ion distribution functions at low temperature. This last assumption may, however, not be exactly valid since the negative ion formation probability (electron capture probability times survival probability) most likely depends on the hydrogen surface-coverage, which changes with temperature. Still, subtracting high from low temperature measurements gives us a distribution function with a reduced backscattering contribution.

Experimentally, it has been observed that, for the energy range studied (50–120 eV), sputtered negative-ion distribution function shapes do almost not depend on the positive ion energy.[61] The same observation is also valid for the backscattering negative ion distribution function shape, except that the high energy tail expands with increasing positive ion energy. It has also been shown that up to a positive ion energy of around 80 eV, 75% of the negative ions measured are created by the sputtering mechanism.[59,61] Above 80 eV, the contribution of sputtering decreases. This decrease has not been explained yet and coincides with a decrease of the total number of the negative ions measured.

III. SRIM CALCULATIONS

SRIM is a group of programs which calculate the stopping and range of ions into matter. SRIM is a Monte-Carlo code based on the binary collision approximation (BCA) which assumes that collisions between atoms can be approximated by binary elastic collisions described by an interaction potential. As discussed by Eckstein *et al.*[72,73] the assumptions underlying the BCA are expected to fail at low particle energy. However, it was empirically proven by the good agreement between experiments and modelling in a vast number of publications (see Ref. 72 and reference therein) that BCA works fine for sputtering calculations despite the fact that in most practical cases the majority of atoms are sputtered in low-energy collisions at the end of the collision cascade. SRIM is able to calculate backscattered and sputtered particle distribution functions resulting from positive atomic-ion bombardment of any amorphous surface. SRIM does not make any statement on the charge of the emitted particles, but as ionization mechanisms are not taken into account in SRIM, it can be thought that SRIM calculations apply first to neutrals. The motivation for using SRIM, even though the present study deals with negative ions, is surface-produced negative ions are basically created by the same mechanisms as surface-produced neutrals, namely the backscattering and the sputtering mechanisms. The only difference is the capture of an electron by the outgoing neutral in the case of negative ions. If the negative ion formation probability is a relatively slowly varying function of the outgoing particle characteristics (type of particle H or D, energy, angle, etc.), then SRIM calculations for neutrals can be used to derive information on negative ion surface creation. The dependence of the formation probability on the outgoing perpendicular velocity is usually strong for metals due to the resonance between the negative-ion affinity-level and the vacant states of the conduction band on the outgoing trajectory. On the contrary, there is not generally such a dependence in insulators where the affinity level crosses the gap on the outgoing trajectory.[74] Therefore, the metallic or nonmetallic character of the plasma-exposed HOPG sample determines the care that has to be taken in using SRIM to interpret negative-ion experiments. This point is discussed at the end of the present paper.

SRIM calculations are only possible for atomic ions impinging on amorphous surfaces. Under the present experimental conditions not only atomic ions impinge the surface but also molecular ions. Most molecular positive ions are neutralized and dissociated upon impact and the energy is shared between the fragments. Therefore, the impact of an H_2^+ ion at energy E_0 can be represented in SRIM calculation by the impact of two H^+ ions at an energy $E_0/2$. For the results presented in this paper, the impact of H_2^+ or D_2^+ and the impact of H_3^+ or D_3^+ are represented in SRIM calculations by H^+ or D^+ impacts at energy respectively equal to $E_0/2$ and $E_0/3$.

Experimentally, HOPG surfaces were used, but upon bombardment, some defects are created in the material and it is partially amorphized[62] up to a depth that depends on the positive ion energy. Furthermore some hydrogen (or deuterium) species are implanted in the material. Therefore, we assumed a dense hydrogenated (deuterated) amorphous carbon material as target in the simulations. A hydrogen (deuterium) and carbon content were taken to be respectively 30% and 70%, which corresponds approximately to the species content of hard a-CH layers.[75] The mass density has been taken from hard a-CH layers as 2.2 g/cm^3.[75]

The surface binding energy, i.e., the minimum energy required to extract an atom from the solid, and the layer density have a strong influence on the calculation results, in

particular on the sputtering yields. Usually, the surface binding energy (E_{sb}) is approximated by the sublimation energy. In the case of hard a-CH (a-CD) layers, surface binding energies for carbon and hydrogen are unknown. Therefore we took the values that were used and justified in previous SRIM calculations (Ref. 75 and reference therein). The carbon surface binding energy has been taken equal to 4.5 eV, a value giving good agreement between observed and calculated sputtering yield.[75] A value of 3 eV has been used for hydrogen and deuterium atoms. The carbon displacement energy, i.e., the energy that an atom has to receive in order to leave its lattice site permanently, has been taken equal to the one of graphite (25 eV), and the hydrogen (deuterium) displacement energy has been taken equal to 2.5 eV. According to Jacob,[75] these values are probably the upper and lower limit for carbon and hydrogen, respectively, in hard a-CH (a-CD) layers. Calculations with increasing E_{sb} values and increasing layer density values were also compared.

To obtain satisfactory statistics in the calculations, the number of ions impinging the surface in normal incidence has been set to 10^5. SRIM then provides backscattered and sputtered NDFs. For low impinging energies considered in the present calculations, almost no carbon atoms are physically sputtered and we focus on hydrogen and deuterium distribution functions.

IV. RESULTS AND DISCUSSION

Experiments and calculations are presented for two sets of experimental data, one in hydrogen, and one in deuterium. For these two experimental conditions the relative densities of the positive ions were measured by mass spectrometry. At 0.4 Pa H_2, 100 W, approximately equal populations of H_2^+ and H_3^+ ions and a negligible H^+ ion population were measured. At 0.2 Pa D_2, 100 W, D_2^+ dominates (around 75%), with the D_3^+ and D^+ fractions being lower. Therefore, the impact of H_2^+ (i.e., H^+ at energy $E_0/2$) and H_3^+ (i.e., H^+ at energy $E_0/3$) ions is considered in the calculations for comparison with experiments at 0.4 Pa H_2, and only D_2^+ (i.e., D^+ at energy $E_0/2$) is considered for comparison with 0.2 Pa D_2.

A. Negative ion maximum energy

The SRIM software allows calculating distribution functions of particles leaving the surface, while the experiments

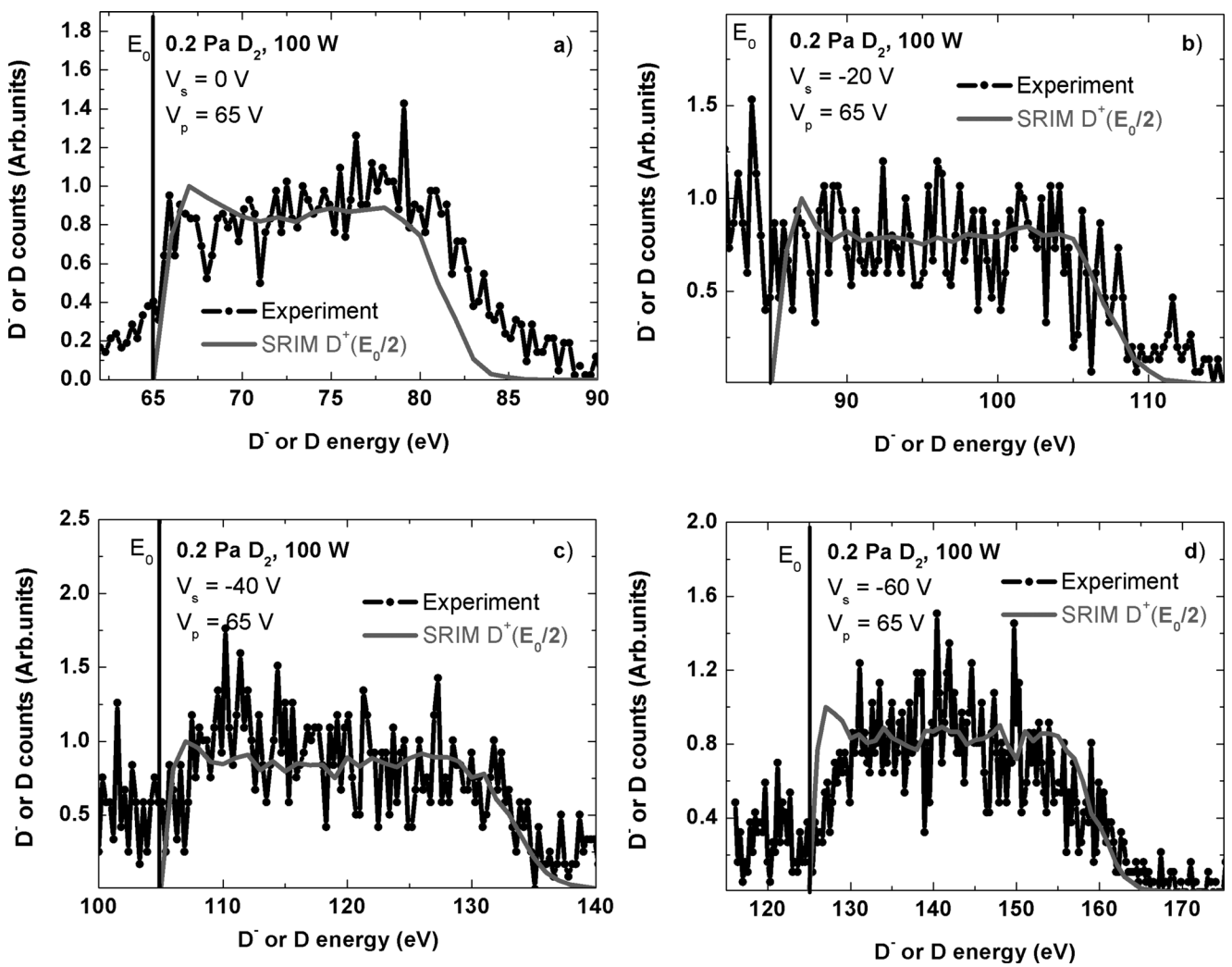

FIG. 2. Comparison between experimental backscattering negative IDFs (lines + symbols) and calculated backscattering neutral distribution functions (lines, a-C layer) in D_2 plasma, 100 W, 0.2 Pa, for different surface biases: (a) 0 V, (b) −20 V, (c) −40 V, (d) −60 V. The IDF maximum energy is always well reproduced by the calculations. The good agreement in the shape is thought to be fortuitous.

allow measuring distribution functions of particles reaching the mass spectrometer detector. Because of the sheath in front of the sample and focusing electrostatic lenses inside the spectrometer, the negative ion transmission between the surface and the mass spectrometer detector is energy and angle dependent. Therefore, a direct comparison between the shapes of the SRIM and the experimental distribution-functions is not possible. Figure 2 shows calculated backscattered-NDFs and measured backscattered-negative-IDFs, all of them normalized to one, in a D_2 plasma at 0.2 Pa and 100 W, and for four positive ion incident energies of $E_0 = 65$, 85, 105, and 125 eV. The NDFs have been shifted by the energy E_0 gained by acceleration through the sheath

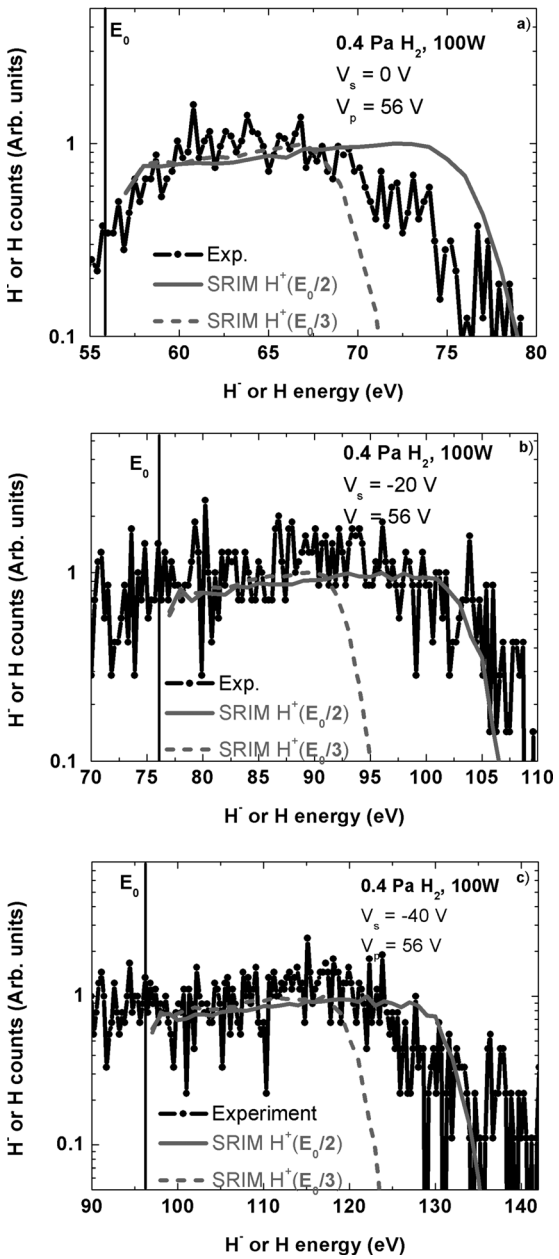

FIG. 3. Comparison between experimental backscattering negative IDFs (lines + symbols) and calculated backscattering neutral distribution functions (full lines and dash lines, a-C layer) in H_2 plasma, 100 W, 0.4 Pa), for different surface bias: (a) 0 V, (b) − 20 V, (c) −40 V. The IDF maximum energy is always well reproduced by the calculations. The good agreement in the shape is thought to be fortuitous.

by the negative ions. This graph permits to compare calculated and measured maximum energy of the distribution functions. The maximum energy of the backscattered IDF is always in good agreement with calculations, confirming that the tail of the IDFs is due to negative ions created by the backscattering mechanism. Surprisingly, the global shape of the backscattered IDFs is correctly reproduced by the calculations. Since the transmission function of the negative ions between the surface and the mass spectrometer should strongly affect the initial distribution function, it is believed this agreement is fortuitous and may be due to the low signal over noise ratio of the experimental results.

Figure 3 presents a comparison between experimental backscattered IDFs and calculated backscattered NDFs shifted by E_0, in H_2 plasma at 0.4 Pa and 100 W and for three positive ion incident energies of $E_0 = 56$, 76, and 96 eV. Two calculations are presented, one for H_2^+ ion impact, and one for H_3^+ impact. These two calculations were not systematically combined to give unique result since the respective percentages of each ion are not accurately known. Maximum energy of backscattered IDFs is well reproduced by the calculations for H_2^+. This confirms that the maximum energy of the IDFs is determined by the lighter non-negligible positive ion. Furthermore it confirms again that the tail of the IDFs is due to negative ions created by the backscattering mechanism. Again, a surprisingly reasonable agreement between IDF and NDF shapes is observed. It is still believed to be fortuitous.

B. Isotopic effect

It was previously observed[61] that the maximum energy of D^- ions is always lower than the maximum energy of H^- ions. This effect was attributed to the higher energy transmitted to the surface by the incoming deuterium ions as compared to the hydrogen ions. This effect is well reproduced by the SRIM calculations as shown in Figure 4 where it can be observed that the maximum energy of the backscattering distribution functions is always lower in the case of deuterium.

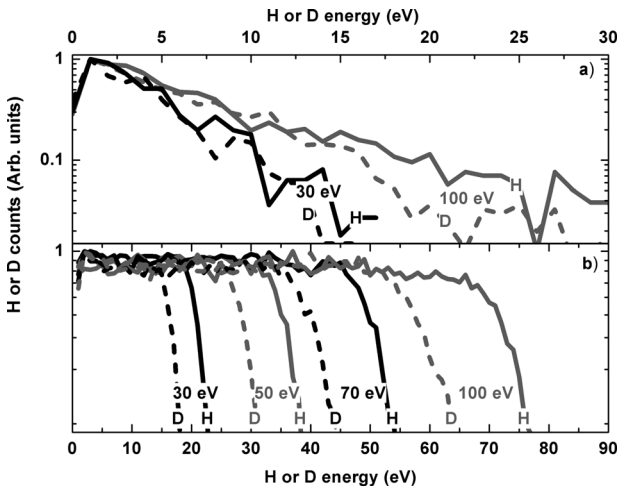

FIG. 4. Comparison between H (full lines) and D (dashed lines) sputtering (a) and backscattering (b) distribution functions calculated by SRIM for different positive ion (H^+ or D^+) impact energies (a-CH and a-CD layers).

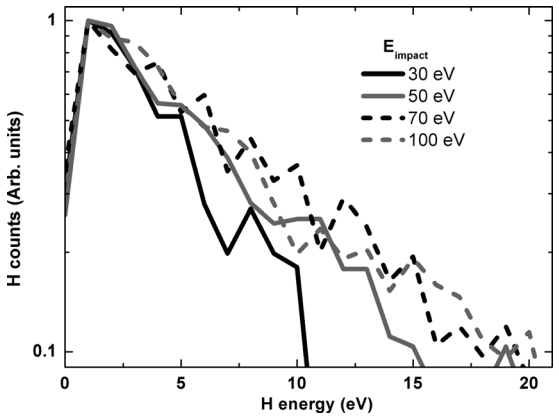

FIG. 5. Comparison between H sputtering distribution functions calculated by SRIM for different positive ion (H^+) impact energies: 30 eV, 50 eV, 70 eV, 100 eV (a-CH layer).

Regarding the sputtering mechanism there is almost no difference between H and D distribution functions.

C. IDF versus positive ion energy

In Figure 5, a comparison is made between calculated sputtered distribution functions for different impinging ion energies. The shapes of these distributions are only weakly dependent on the positive ion energy, at least for energies varying by a few tens of volts, as we already observed experimentally in Ref. 59, and had already been observed previously.[76,77] However, the energy of the impinging positive ion is primordial to reproduce correctly the maximum energy of the backscattered IDFs (see Figure 3).

D. Negative ion yields

In Figure 6, the calculated backscattering and sputtering contributions are presented versus positive-ion energy together with the estimated experimental contributions. There is a strong disagreement between the experiments and calculations. The calculated neutral backscattering contribution is always much higher than the sputtering one, in contradiction with negative-ion experiments. From SRIM results, more than

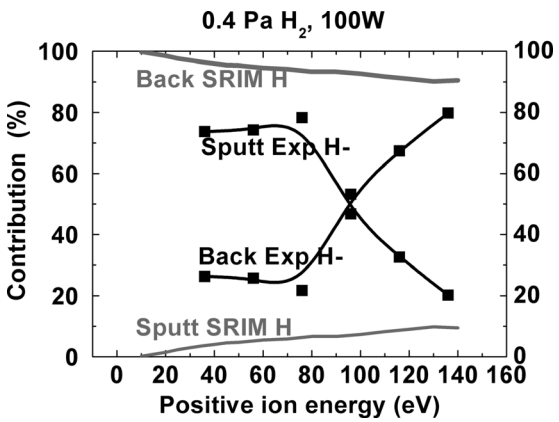

FIG. 6. Sputtering and backscattering contributions to the total H^- surface-production, as estimated from the experiments (full lines + squares), versus H_2^+/H_3^+ positive ion energy. Sputtering and backscattering contributions to the total H surface emission as calculated by SRIM (full lines), versus H^+ positive ion impact energy (a-CH layer).

90% of the particles emitted by the surface originate from the backscattering mechanism, while in the experiments sputtering contribution is dominating up to a positive ion energy of around 80 eV. Plotting the experimental results versus the energy per nucleon ($E_0/2$ for H_2^+ impact and $E_0/3$ for H_3^+ impact) instead of the positive-ion energy (E_0) would not change the observations made.

First of all, an overestimation of the sputtering contribution in the experiments cannot be excluded, as in order to derive this result the assumption has been made that the electron capture is temperature independent (see Sec. II). Hence, the difference between experiments and calculations may not be as important as observed on Figure 6. However, from the general shape of the measured IDFs, and from the strong decrease of the low energy part of the IDFs when surface coverage decreases (temperature increases), it is obvious that sputtered negative ions are much more numerous than backscattered negative-ions. Therefore, an overestimation of the sputtering contribution in the experiments is probable but cannot account for such a difference between experiments and calculations.

Second, the sample roughness, which leads to a change of the effective angle of incidence, is not taken into account in the calculations. Kuestner *et al.*[78] have studied the influence of surface roughness on the sputtering yield of D^+ ion impinging on pyrolitic graphite (HOPG) or isotropic graphite (EK98), taking into account the effective distribution of angles of incidence as measured by STM. For an initially rough surface of isotropic graphite (EK98) and normal incidence, roughness has a strong influence on the sputtering yield. On the contrary, for an initially flat HOPG surface, roughness has a weak influence on the sputtering yield at normal incidence (the distribution of real angles of incidence is not large and is peaked close to the normal, at 15°). Furthermore, Mayer *et al.*[79] have shown that backscattering is not strongly influenced by roughness in the case of an initially flat HOPG surface (HOPG) bombarded by D^+ ions. In the present experiments we have an initially flat HOPG surface and the ion incidence is normal. It is thus expected that taking into account the real distribution of incidence angles as in Ref. 78, would only lead to slight changes of the calculated yields. Furthermore, SRIM calculations performed for hydrogen impact at 75 eV on a-CH layer at different angles of incidence, show that the sputtering contribution is only varying by 1% over the entire range of angles (0° to 80° with 10° steps). The sputtering yield actually increases with angle of incidence but so does the backscattering yield, resulting in an almost constant contribution of sputtering. Therefore, the disagreement between calculations and experiments is not related to the surface roughness.

A difference in the electron capture probability for the two mechanisms is to be excluded since whatever the mechanism, the particles leaving the surface are in the same energy range except for the tail of the backscattering distribution function.

Finally, to obtain a more satisfactory explanation, one has to consider the angular distribution of the surface-emitted particles. SRIM can provide the angular distribution of particles emitted from the surface. This distribution is

presented for H and D atoms for two positive ion energies (H^+ and D^+ ions at 50 and 100 eV), for the sputtering (lines in Figure 7(a)) and the backscattering (lines in Figure 7(b)) processes. In Figures 7(a) and 7(b), the normalized energy (energy divided by the impact energy) of the emitted particles is plotted versus the emission angle (black dots). The first observation is that the maximum energy of the emitted particles is much higher for the backscattering process than for the sputtering process.

From Figures 7(a) and 7(b), one can also see that the angular dependence of both processes (lines on figures) hardly depends on the impact energy (50 eV top plots, 100 eV bottom plots) and on the particle considered (H, left column or D, right column). On the other hand, the angular emission yield is strongly dependent on the process considered. Concerning sputtering, the emission yield shows a maximum at 20° and goes to zero above 45°. Concerning backscattering, the yield is maximal at 45° and goes to zero above 70°.

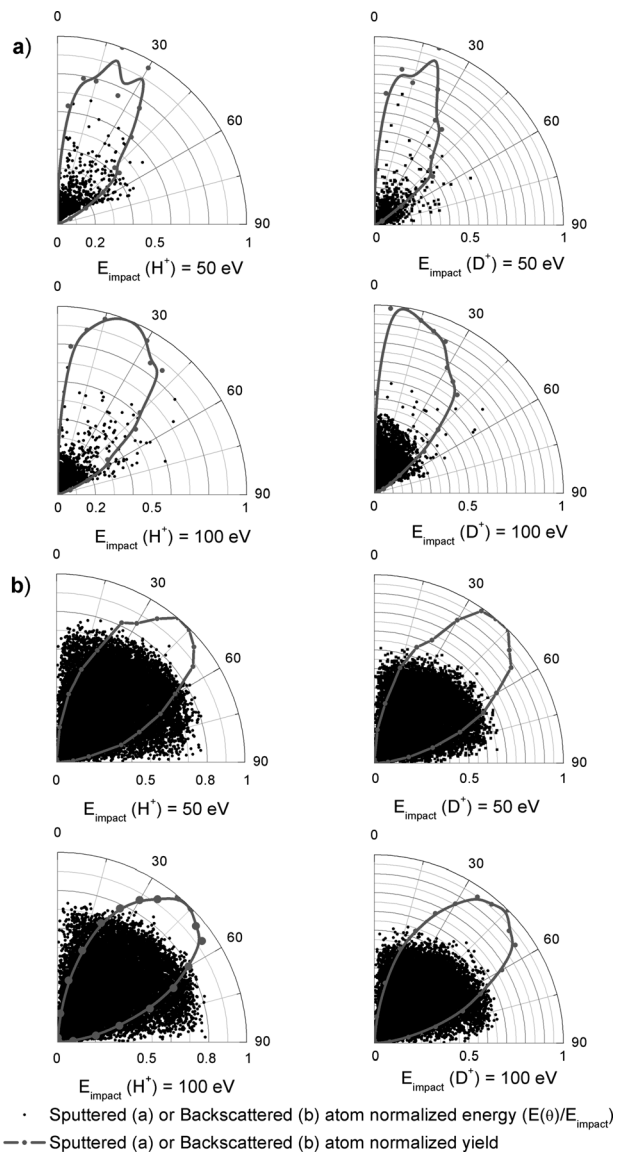

FIG. 7. Black dots: Polar plot of the sputtered (a) or backscattered (b) atom (H on left, D on right) normalized energy ($E_{emission}$(atom)/E_{impact} (positive ion)) for two impact energies: 50 eV (top) and 100 eV (bottom). Grey line: Polar plot of the sputtered (a) or backcscattered (b) atom (H on left, D on right) normalized yield ($N_{sputtered}(\theta)/N_{sputtered}(\theta_{max})$) for two impact energies: 50 eV (top) and 100 eV (bottom). 0° is the direction normal to the surface. a-CH and a-CD layers.

The negative ion trajectories are rectified by the sheaths, one in front of the sample and one in front of the mass spectrometer. To be detected, negative ions must enter the mass spectrometer close to normal incidence as the acceptance angle is on the order of a few degrees.[80] For a given energy, the lower the angle of emission is, the closer the incidence angle for the mass spectrometer is to the normal and, hence, the higher the detection probability. As sputtered particles are emitted at lower angle, their collection by the mass spectrometer is favoured compared to that of the backscattered particles, leading to a distribution function where sputtered particles dominate. The same phenomenon was already observed on barium surfaces.[66] An exact calculation of negative ion transmission through sheaths cannot be undertaken easily since the sheath shape around the sample and the mass spectrometer nozzle are unknown (the biased sample is surrounded by a floating ceramic surface and the biased mass-spectrometer entrance hole is surrounded by a grounded surface, leading to complex sheath shapes). We reserve such calculations for the future. However, it is obvious that particles emitted at lower angle have a higher probability to be collected by the mass spectrometer since their trajectories are easily rectified by the electric field in the sheath. As the sputtered particle distribution is peaked at lower angle, it explains that relatively more sputtered negative-ions are detected than backscattered negative-ions. The difference in the calculated and experimental contributions in Figure 6 can be seen as an illustration of the difference between surface-produced negative-ion distribution functions and measured negative-ion distribution functions, rather than a disagreement between calculations and experiments. Calculations concern particles emitted by the surface, while the experiments measure negative ions that are able to reach the mass spectrometer detector. Interestingly, it also suggests that many negative ions emitted by the surface are not collected, and that carbon is probably an even better negative ion enhancer than previously thought.[62]

Figure 6 also shows that above 80 eV the sputtering contribution starts to decrease. This is in contradiction with the calculations where the sputtering contribution always increases while the backscattering one always decreases for positive ion energy varying from 20 eV to 120 eV and the backscattering remains higher than the sputtering contribution by at least a factor 7. SRIM calculations do not include any modification of the surface upon positive-ion bombardment. As the positive-ion energy increases, the hydrogen or deuterium surface coverage might decrease and lead to a decrease of the sputtering contribution to negative ion formation. We have estimated this effect using SRIM yields and a system of rate equations to calculate the steady-state hydrogen coverage and found that it is negligible compared to the strong decrease found experimentally. We have no clear explanation at the moment concerning the decrease of the sputtering contribution, but we think it may come from negative-ion collection issues with increasing ion energies.

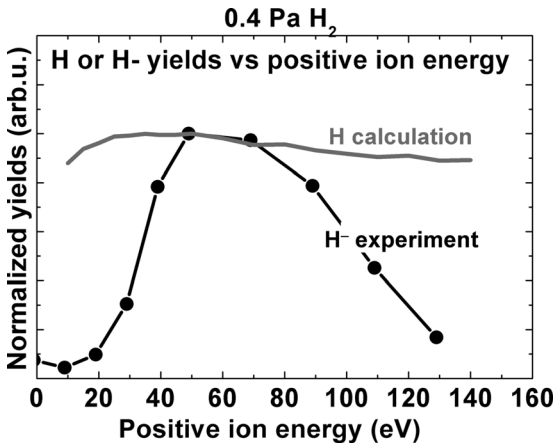

FIG. 8. H (grey line) and H^- (black line and full circles) yields versus H^+ positive ion impact energy (calculations) and versus H_2^+/H_3^+ positive ion energy (experiments). Yield is defined as the total number of events (backscattering plus sputtering) divided by the total number of impinging positive ions.

Figure 8 presents the normalized total yield for neutral production (SRIM) and for negative ion production.[60] The yield is defined as the total number of events (backscattering plus sputtering) divided by the total number of impinging positive ions. One can see that the calculated yield hardly depends on the positive ion energy (only 10% variation between 10 and 150 eV) while the measured yield strongly depends on the positive ion energy. Indeed a marked decrease of the measured yield is observed above 80 eV. Again, plotting the experimental results versus the energy per nucleon ($E_0/2$ for H_2^+ impact and $E_0/3$ for H_3^+ impact) instead of the positive-ion energy (E_0) would not change the observations made. The cause of this disagreement between SRIM and experiments is not clear up to now. However, it can be observed that this decrease is concomitant with the decrease of the sputtering contribution (Figure 6). Therefore, it is likely that the previously discussed negative-ion transmission and collection issues play a role when the energy is increased. The strong increase of the experimental yield at low positive ion energy is due to the onset of the sputtering mechanisms. SRIM results show only a slight increase since sputtering has a low contribution to the total yield in the calculations.

The previous discussions about collection issues show that the present experimental arrangement could not be used as it is in a self-extracted negative-ion source.[66,81] Angular distributions of emitted particles imply that the graphite surface, if used as a surface converter, would have to be concave to focus the negative-ions towards the exit, as was done in the past by Ehlers *et al.*[81] Also, the surface conversion principle leads to negative-ion beams with large energy spread and large emittance. In a real ion source structure, ion extraction apertures, focusing devices (like quadrupoles), dipole magnets (to analyze the energy) along with post slits could be used to reduce the beam emittance and energy spread. However, the primary objective of the present work is not to design a negative-ion source, but rather to understand surface production in cesium-free plasmas by analyzing negative-ion distribution functions (this work), and by comparing them for different materials.[62]

TABLE I. Calculated backscattering and sputtering yields for different SRIM input parameters. "Esb" is the surface binding energy. "%H or D" is the hydrogen or deuterium percentage in the a-CH or a-CD layer considered.

	Backscattering yields		Sputtering yields	
Species	H	D	H	D
$E_{sb} = 0.5$ eV	0.2	0.16	3.2E-02	2.6E-02
$E_{sb} = 1.5$ eV	0.2	0.16	1.9E-02	1.4E-02
$E_{sb} = 3.0$ eV	0.2	0.16	1.0E-02	6.0E-03
$E_{sb} = 4.5$ eV	0.2	0.16	6.0E-03	3.0E-03
%H or D = 0%	0.26	0.2	0.0E + 00	0.0E + 00
%H or D = 20%	0.22	0.17	5.0E-03	3.5E-03
%H or D = 30%	0.2	0.16	1.0E-02	6.0E-03
%H or D = 40%	0.17	0.14	1.6E-02	9.5E-03
%H or D = 50%	0.15	0.12	2.0E-02	1.5E-02

E. Other SRIM input parameters

SRIM calculations were also performed with different input parameters, as summarized in Table I. The surface binding energy and the percentage of deuterium or hydrogen on the surface were varied for positive ion impact energy of 50 eV. Both parameters influence the sputtering yield, which increases when the surface binding energy decreases from 4.5 to 0.5 eV (yields from 0.003 to 0.026 in D_2 and from 0.006 to 0.032 in H_2) and when the deuterium or hydrogen percentage increases from 20% to 50% (yield from 0.003 to 0.014 in D_2 and from 0.005 to 0.02 in H_2). As expected, the backscattering yield is not influenced by the surface binding energy but decreases when the deuterium or hydrogen coverage increases from 0% to 50% (yield from 0.26 to 0.15 in H_2 and from 0.2 to 0.12 in D_2). In any condition, the backscattering yield remains much higher than the sputtering yield. The shapes of the distribution functions are essentially not influenced by these two parameters. Interestingly one can see that backscattering and sputtering yields are always lower in deuterium (which means that the deuterium implantation yield is higher). One can also note from Table I that the backscattering yield is not constant with H/D surface coverage. There is a 20% variation of the yield when the surface coverage decreases from 30% (coverage expected at room temperature) to 0% (coverage expected at high temperature). Therefore, even without any consideration on the electron capture dependence with coverage, the assumption we made in Ref. 61 (backscattering yield is constant with temperature) is not strictly correct.

Finally, calculations were performed with varying layer densities of an a-CD layer at an impact energy of 50 eV. The backscattering yield is not influenced by the layer density while the sputtering yield slightly increases from 0.005 to 0.006 when the layer density increases from 1.3 g/cm^3 to 2.2 g/cm^3.

F. Negative ion formation probability

The probability of the surface formation of negative ions is in general dependent upon the trajectory of the outgoing particle (perpendicular velocity, outgoing angle, outgoing total energy, etc.). This has been shown in beam

experiments for several cesiated and non-cesiated, metallic surfaces.[22,30,31] However, regarding graphite, Gleeson and Kleyn[38] did not observe any clear dependence of the negative ion yield versus the outgoing angle in beam experiments where 300 eV H_2^+ ions where impinging on a HOPG surface with a 70° incidence angle. The HOPG behaviour was in that sense very similar to the diamond behaviour (large band-gap of 5.5 eV) and very different from the metallic behaviour of the barium-dosed diamond. Recent experiments performed at ISMO laboratory (Paris-Sud University) reinforced the idea of the non-metallic behaviour of graphite with respect to the negative-ion surface formation.[82] In Ref. 37, it was not observed any dependence of the negative-ion yield with the outgoing angle (between 0° and 70°), for 400 eV H_2^+ and H_3^+ positive-ion impacting on HOPG with an incidence angle of 70°. In a higher energy beam experiment, Vidal *et al.*[40] observed almost no dependence of the H– yield for outgoing angles between 55° and 70° when a 4 keV H^+ beam is impinging on HOPG surface with an incident angle of 22.5° (700 eV perpendicular velocity). It can be concluded that, based on published beam-experiment results, it appears reasonable to assume that the negative-ion formation probability (including both capture and survival probabilities) does not strongly depend on the outgoing particle energy and angle in the case of hydrogen positive-ions impinging on HOPG surfaces.

V. CONCLUSION

In previous works, we have studied negative ion surface-production in H_2 and D_2 plasmas on a graphite surface (HOPG). It has been experimentally demonstrated that negative ions are created via two mechanisms: (i) backscattering of a positive ion as a negative ion and (ii) sputtering of an adsorbed atom as a negative ion. The dependence of the negative ion yield versus positive ion energy and type was established.

In the present paper, backscattered and sputtered particles distribution-functions, arising from hydrogen (deuterium) positive-ion bombardment of an a-CH(D) layer were computed using the SRIM software in order to obtain a better understanding of the experimentally measured negative-ion distributions. As all the physics behind the measurements is not included in the SRIM calculations, a direct comparison between calculations and experiments is not possible. However, SRIM calculations proved useful as a support for the interpretation of the experiments. In particular, it has been shown that SRIM calculations are in good agreement with negative-ion experiments concerning the maximum energy of the outgoing particle and its isotopic dependence. This is particularly important since it was previously deduced that negative ions are formed by the backscattering mechanism by considering this maximum energy under various experimental conditions.[60,61] This deduction is thus fully validated.

Yield-calculations are not in good agreement with experiments. While it is calculated that backscattered particles largely dominate, a higher proportion of negative ions created by the sputtering mechanism is measured. An explanation is proposed based on the emitted-particle angular distributions calculated by SRIM. Sputtered negative ions are collected more efficiently because they are emitted from the surface closer to the normal than backscattered ions, and thus they have a higher probability to reach the mass spectrometer at an angle smaller than the maximum acceptance angle. There is still a major difference between calculations and experiments regarding yields. Negative-ion surface-production strongly decreases for positive-ion energies above 80 eV while calculations do not predict such a big change. It is believed to be due to a negative-ion collection issue. As it is now shown that SRIM can be used to interpret negative-ion experiments under the present experimental conditions, we plan to model in the future negative-ion trajectories between the surface and the mass spectrometer, based on outgoing-particle energies and angles determined by SRIM.

ACKNOWLEDGMENTS

This work, supported by the European Communities under the contract of Association between EURATOM, CEA, and the French Research Federation for fusion studies, was carried out within the framework of the European Fusion Development Agreement. The views and opinions expressed herein do not necessarily reflect those of the European Commission. Financial support was also received from the French Research Agency (ANR) under Grant ITER-NIS (ANR-08-BLAN-0047) "ITER-Negative Ion Sources," and Department of Science and Technology (DST), India under BOYSCAST fellowship program. Hocine Khemliche (ISMO, Paris-Sud University) is acknowledged for the fruitful discussions we had about negative-ion surface formation.

[1]E. Speth, H. D. Falter, P. Franzen, U. Fantz, M. Bandyopadhyay, S. Christ, A. Encheva, M. Fröschle, D. Holtum, B. Heinemann, W. Kraus, A. Lorenz, Ch. Martens, P. McNeely, S. Obermayer, R. Riedl, R. Süss, A. Tanga, R. Wilhelm, and D. Wünderlich, Nucl. Fusion **46**, S220 (2006).
[2]P. McNeely and L. Schiesko, Rev. Sci. Instrum. **81**, 02B111 (2010).
[3]D. Wünderlich, R. Gutser, and U. Fantz, Plasma Sources Sci. Technol. **18**, 045031 (2009).
[4]J. P. Boeuf, G. J. M. Hagelaar, P. Sarrailh, G. Fubiani, and N. Kohen, Plasma Sources Sci. Technol. **20**, 015002 (2011).
[5]G. J. M. Hagelaar, G. Fubiani, and J.-P. Boeuf, Plasma Sources Sci. Technol. **20**, 015001 (2011).
[6]V. Dudnikov, P. Chapovsky, and A. Dudnikov, Rev. Sci. Instrum. **81**, 02A714 (2010).
[7]L. Schiesko, P. McNeely, U. Fantz, P. Franzen, and NNBI Team, Plasma Phys. Controlled Fusion **53**, 085029 (2011).
[8]P. Franzen, L. Schiesko, M. Fröschle, D. Wünderlich, U. Fantz, and the NNBI Team, Plasma Phys. Controlled Fusion **53**, 115006 (2011).
[9]P. Svarnas, B. M. Annaratone, S. Béchu, J. Pelletier, and M. Bacal, Plasma Sources Sci. Technol. **18**, 045010 (2009).
[10]S. Mochalskyy, A. F. Lifschitz, and T. Minea, Nucl. Fusion **50**, 105011 (2010).
[11]F. Taccogna, P. Minelli, S. Longo, M. Capitelli, and R. Schneider, Phys. Plasmas **17**, 063502 (2010).
[12]Yu. I. Belchenko, G. I. Dimov, and V. G. Dudnikov, Nucl. Fusion **14**, 113 (1974).
[13]R. S. Hemsworth and T. Inoue, IEEE Trans. Plasma Sci. **33**, 1799 (2005).
[14]S. Bechu, D. Lemoine, M. Bacal, A. Bes, and J. Pelletier, AIP Conf. Proc. **1097**, 74–83 (2009).
[15]M. Capitelli, M. Cacciatore, R. Celiberto, O. De Pascale, P. Diomede, F. Esposito, A. Gicquel, C. Gorse, K. Hassouni, A. Laricchiuta, S. Longo, D. Pagano, and M. Rutigliano, Nucl. Fusion **46**, S260–S274 (2006).
[16]M. Bacal, Nucl. Fusion **46**, S250–S259 (2006).
[17]F. Taccogna, R. Schneider, K. Matyash, S. Longo, M. Capitelli, and D. Tskhakaya, J. Nucl. Mater. **363–365**, 437–442 (2007).

[18]S. Kado, S. Kajita, D. Yamasaki, Y. Iida, B. Xiao, T. Shikama, T. Oishi, A. Okamoto, and S. Tanaka, J. Nucl. Mater. **337–339**, 166–170 (2005).
[19]A. Tonegawa, M. Ono, Y. Morihira, H. Ogawa, T. Shibuya, K. Kawamura, and K. Takayama, J. Nucl. Mater. **313–316**, 1046–1051 (2003).
[20]H. Gnaser, Appl. Surf. Sci. **203**, 78 (2003)
[21]H. Gnaser, Nucl. Instrum. Methods Phys. Res. B **164**, 705 (2000).
[22]J. R. Hiskes and P. J. Schneider, Phys. Rev. B **23**, 949 (1981).
[23]M. Seidl, H. L. Cui, J. D. Isenberg, H. J. Kwon, B. S. Lee, and S. T. Melnychuk, J. Appl. Phys. **79**(6), 15 (1996).
[24]M. Seidl and A. Pargellis, Phys. Rev. B **26**, 1 (1982).
[25]L. Yu. Ming, Phys. Rev. Lett. **40**, 574 (1978).
[26]H. Verbeek, W. Eckstein, and R. S. Bhattacharya, Surf. Sci. **95**, 380–390 (1980).
[27]J. Schneider, W. Eckstein, and H. Verbeek, Nucl. Instrum. Methods Phys. Res. B **218**, 713 (1983).
[28]P. Roncin, A. G. Borisov, H. Khemliche, A. Momeni, A. Mertens, and H. Winter, Phys. Rev. Lett. **89**, 043201 (2002).
[29]A. G. Borisov, V. Sidis, P. Roncin, A. Momeni, H. Khemliche, A. Mertens, and H. Winter, Phys. Rev. B **67**, 115403 (2003).
[30]M. Maazouz, L. Guillemot, V. A. Esaulov, and D. J. O'Connor, Surf. Sci. **398**, 49–59 (1998).
[31]M. Maazouz, A. G. Borisov, V. A. Esaulov, J. P. Gauyacq, L. Guillemot, S. Lacombe, and D. Teillet-Billy, Phys. Rev. B **55**, 13869 (1997).
[32]M. A. Gleeson, M. Kropholler, and A. W. Kleyn, Appl. Phys. Lett. **77**(8), 21 (2000).
[33]J. A. Scheer, M. Wieser, P. Wurz, P. Bochsler, E. Hertzberg, S. A. Fuselier, F. A. Koeck, R. J. Nemanich, and M. Schleberger, Nucl. Instrum. Methods Phys. Res. B **230**, 330–339 (2005).
[34]R. Souda, E. Asari, H. Kawanowa, T. Suzuki, and S. Otani, Surf. Sci. **421**, 89–99 (1999).
[35]S. G. Walton, R. L. Champion, and Y. Wang, J. Appl. Phys. **84**(3), 1 (1998).
[36]A. G. Borisov and V. A. Esaulov, J. Phys.: Condens. Matter **12**, R177 (2000).
[37]K. Tsumori, W. R. Koppers, R. M. A. Heeren, M. F. Kadodwala, J. H. M. Beijersbergen, and A. W. Kleyn, J. Appl. Phys. **81**, 6390 (1997).
[38]M. A. Gleeson and A. W. Kleyn, Nucl. Instrum. Methods Phys. Res. B **157**, 48–54 (1999).
[39]F. Bonetto, E. A. García, R. Vidal, J. Ferron, and E. C. Goldberg, Appl. Surf. Sci. **254**, 62–64 (2007).
[40]R. A. Vidal, F. Bonetto, J. Ferrón, M. A. Romero, E. A. García, and E. C. Goldberg, Surf. Sci. **605**, 18–23 (2011).
[41]T. Hayashi, S. Murai, F. Sato, A. Kono, N. Mizutani, and K. Suu, Jpn. J. Appl. Phys., Part 1 **50**(8), 08KB01 (2011).
[42]H. Oomori, T. Kasuya, M. Wada, Y. Horino, and N. Tsubouchi, Rev. Sci. Instrum. **71**(2), 1123 (2000).
[43]Th. Welzel, S. Naumov, and K. Ellmer, J. Appl. Phys. **109**, 073302 (2011).
[44]N. Ito, N. Oka, Y. Sato, and Y. Shigesato, Jpn. J. Appl. Phys., Part 1 **49**, 071103 (2010).
[45]J. M. Andersson, E. Wallin, E. P. Münger, and U. Helmersson, J. Appl. Phys. **100**, 033305 (2006).
[46]J.-P. Krumme, R. A. A. Hack, and I. J. M. M. Raaijmakers, J. Appl. Phys. **70**, 6743 (1991).
[47]S. Mahieu, W. P. Leroy, K. Van Aeken, and D. Depla, J. Appl. Phys. **106**, 093302 (2009).
[48]S. Mahieu and D. Depla, Appl. Phys. Lett. **90**, 121117 (2007).
[49]S. Mráz and J. M. Schneider, Appl. Phys. Lett. **89**, 051502 (2006).
[50]S. Mráz and J. M. Schneider, J. Appl. Phys. **100**, 023503 (2006).
[51]K. Tominaga and T. Kikuma, J. Vac. Sci. Technol. A **19**, 1582 (2001).
[52]H. Toyoda, K. Goto, T. Ishijima, T. Morita, N. Ohshima, and K. Kinoshita, Appl. Phys. Express **2**, 126001 (2009).
[53]T. Ishijima, K. Goto, N. Ohshima, K. Kinoshita, and H. Toyoda, Jpn. J. Appl. Phys., Part 1 **48**, 116004 (2009).
[54]N. Tsukamoto, D. Watanabe, M. Saito, Y. Sato, N. Oka, and Y. Shigesato, J. Vac. Sci. Technol. A **28**, 846 (2010).
[55]T. Welzel, R. Kleinhempel, T. Dunger, and F. Richter, Plasma Processes Polym. **6**, S331–S336 (2009).
[56]F. Richter, T. Welzel, R. Kleinhempel, T. Dunger, T. Knoth, M. Dimer, and F. Milde, Surf. Coat. Technol. **204**, 845–849 (2009).
[57]M. Zeuner, H. Neumann, J. Zalman, and H. Biederman, J. Appl. Phys. **83**(10), 5084 (1998).
[58]R. Wendt and K. Ellmer, Surf. Coat. Technol. **93**, 27–31 (1997).
[59]L. Schiesko, M. Carrère, J.-M. Layet, and G. Cartry, Appl. Phys. Lett. **95**, 191502 (2009).
[60]L. Schiesko, M. Carrère, G. Cartry, and J.-M. Layet, Plasma Sources Sci. Technol. **17**, 035023 (2008).
[61]L. Schiesko, M. Carrère, J.-M. Layet, and G. Cartry, Plasma Sources Sci. Technol. **19**, 045016 (2010).
[62]P. Kumar, A. Ahmad, C. Pardanaud, M. Carrère, J.-M. Layet, G. Cartry, F. Silva, A. Gicquel, and R. Engeln, J. Phys. D: Appl. Phys. **44**, 372002 (2011).
[63]T. Babkina, T. Gans, and U. Czarnetzki, Europhys. Lett. **72**, 235–241 (2005).
[64]C. F. A. Van Os, R. M. A. Heeren, and P. W. Vanamersfoort, Appl. Phys. Lett. **51**, 1495–1497 (1987).
[65]R. M. A. Heeren, D. Ciric, S. Yagura, H. J. Hopman, and A. W. Kleyn, Nucl. Instrum. Methods Phys. Res. B **69**, 389–402 (1992).
[66]C. F. A. van Os, P. W. van Amersfoort, and J. Los, J. Appl. Phys. **64**, 3863 (1988).
[67]R. M. A. Heeren, M. J. de Graaf, D. Ciric, H. J. Hopman, and A. W. Kleyn, J. Appl. Phys. **75**, 4340 (1994).
[68]R. M. A. Heeren, M. J. de Graaf, D. Ćirić, H. J. Hopman, and A. W. Kleyn, Appl. Surf. Sci. **70-71**, 332–336 (1993).
[69]J. F. Ziegler, J. P. Biersack, and M. D. Ziegler, *SRIM—The Stopping and Range of Ions in Matter* (SRIM Co., 2008), ISBN 0-9654207-1-X.
[70]V. Kaeppelin, M. Carrère, and J. B. Faure, Rev. Sci. Instrum. **72**, 4377 (2001).
[71]V. Kaeppelin, M. Carrère, and J.-M. Layet, Plasma Sources Sci. Technol. **11**, 53–56 (2002).
[72]W. Eckstein and H. M. Urbassek, *Sputtering by Particle Bombardment, Topics in Applied Physics* Vol. 110 (Springer, 2007), p. 24.
[73]W. Eckstein, *Computer Simulation of Ion Solid Interactions, Springer Series in Materials Science*, Vol. 10 (Springer, Berlin, 1991).
[74]A. G. Borisov and V. Sidis, Phys. Rev. B **56**(16), 10628 (1997).
[75]W. Jacob, Thin Solid Films **326**, 1–42 (1998).
[76]A. Goehlich, D. Gillman, and H. F. Döbele, Nucl. Instrum. Methods Phys. Res. B **164–165**, 834–839 (2000).
[77]A. Goehlich, Niemöller, and H. F. Döbele, Phys. Rev. B **62**, 9349 (2000).
[78]M. Kustner, W. Eckstein, V. Dose, and J. Roth, Nucl. Instrum. Methods Phys. Res. B **145**, 320 (1998).
[79]M. Mayer, W. Eckstein, and B. M. U. Scherzer, J. Appl. Phys. **77**, 6609 (1995).
[80]M. H. S. Low, C. H. A. Huan, A. T. S. Wee, and K. L. Tan, Nucl. Instrum. Methods Phys. Res. B **103**, 482–488 (1995).
[81]K. W. Ehlers and K. N. Leung, Rev. Sci. Instrum. **51**(6), 721 (1980).
[82]Private communication, ISMO laboratory, Paris-Sud University - CNRS, 2012.